



UNIVERSITY OF LEEDS

This is a repository copy of *Two-Stage Thermoacoustic Electricity Generator for Waste Heat Recovery*.

White Rose Research Online URL for this paper:
<http://eprints.whiterose.ac.uk/99365/>

Version: Accepted Version

Proceedings Paper:

Hamood, A, Mao, X orcid.org/0000-0002-9004-2081 and Jaworski, AJ (2016) Two-Stage Thermoacoustic Electricity Generator for Waste Heat Recovery. In: Ao, SI, Gelman, L, Hukins, DWL, Hunter, A and Korsunsky, AM, (eds.) Proceedings of World Congress on Engineering 2016. World Congress on Engineering 2016, 29 Jun - 01 Jul 2016, London, UK. International Association of Engineers , pp. 944-949. ISBN 978-988-14048-0-0

This is an author produced version of a conference paper accepted for publication in the Proceedings of World Congress on Engineering 2016. Uploaded with permission from the publisher.

Reuse

Items deposited in White Rose Research Online are protected by copyright, with all rights reserved unless indicated otherwise. They may be downloaded and/or printed for private study, or other acts as permitted by national copyright laws. The publisher or other rights holders may allow further reproduction and re-use of the full text version. This is indicated by the licence information on the White Rose Research Online record for the item.

Takedown

If you consider content in White Rose Research Online to be in breach of UK law, please notify us by emailing eprints@whiterose.ac.uk including the URL of the record and the reason for the withdrawal request.



eprints@whiterose.ac.uk
<https://eprints.whiterose.ac.uk/>

Two-Stage Thermoacoustic Electricity Generator for Waste Heat Recovery

Ahmed HAMOOD, Xiaoan MAO, Artur J. JAWORSKI

Abstract— This paper presents the design, construction and tests of a two-stage traveling-wave thermoacoustic electricity generator. The engine designed has two stages with a Linear Alternator connected in between two points having equal but out of phase acoustic pressure amplitudes. The connection of Linear Alternator in this configuration allows it to be run by the effect of acoustic pressure on both sides and work in a "push-pull" mode. Pressurized helium at 28 bar is used as working gas and operating frequency is 54.68 Hz. In the experiments, a maximum generated electricity and thermal-to-electric efficiency of 48.6 W and 2.7% are obtained, respectively, when the temperature difference across the regenerator reaches 300°C at 30.8 Ω load resistance. The research results shown in this paper demonstrate that two identical half-wave length stages can run a linear alternator in "push-pull" mode.

Index Terms— Electricity generator, push-pull, thermoacoustic, traveling wave

I. INTRODUCTION

Day by day, power demand rises all over the world. In the last decades, a lot of environmental impacts have been found and proven as caused by the power generation technologies. This creates a thinking approach towards clean and environmentally friendly technologies. Thermoacoustic power generation technology could be considered as one of such technologies.

The working principle of thermoacoustic devices is based on a thermoacoustic effect which enables producing sound waves from thermal energy, or vice-versa. Thermoacoustic devices are generally described as acoustic resonators filled with a gas as a working fluid and containing a porous medium (regenerator) with heat source and heat sink (heat exchangers) adjacent to it. The gas inside the resonance tube (within the porous medium limits) will undergo a thermodynamic cycle somewhat similar to the Stirling cycle. In thermoacoustic engine, the working gas absorbs heat from high temperature side of the porous medium and rejects heat to the low temperature side while producing work in the form of sound oscillations as an output.

Manuscript received March 6, 2016; revised April 16, 2016. This work was supported in part by the Human Capacity Development Program (HCDP) sponsored by Kurdistan regional government (A. Hamood) and in part by the Royal Society Industry Fellowship (A.J. Jaworski)

Ahmed Hamood is with the Faculty of Engineering, University of Leeds, Leeds LS2 9JT, UK; (email: mnamh@leeds.ac.uk).

Xiaoan Mao is with the Faculty of Engineering, University of Leeds, Leeds LS2 9JT, UK; (email: x.mao@leeds.ac.uk).

Artur J. Jaworski, the corresponding author, is with the Faculty of Engineering, University of Leeds, Leeds LS2 9JT, UK; (email: a.j.jaworski@leeds.ac.uk).

Looped tube thermoacoustic engine is one of the simplest traveling wave configurations and consists of long resonator (one or more wave lengths) which contains the regenerator unit and the Linear Alternator. Investigations of a looped tube thermoacoustic system have been done by Sakamoto et al. (2006, 2012). These investigations have been done on a combined thermoacoustic engine and refrigerator. Using air as a working gas, the system gave a cooling power at cooling efficiency of about 0.15 W and 0.13%, respectively. They subsequently improved performance to reach 0.8 W of cooling power and 1.5% of cooling efficiency, by using a mixture of helium and argon (50:50) instead of air.

The looped engine configuration has also been used in SCORE project. Thermoacoustic engine was found to be able to convert waste heat from the cooking stove to electricity. The engine has been made of commercially available materials and air at atmospheric pressure has been used as working fluid (Yu et al., 2012). The simulated efficiencies of thermal to acoustic, acoustic to electric and thermal to electric conversion were 4.6%, 53% and 2.4%, respectively producing electricity of 8 W. Abdoulla et al. (2013) subsequently improved the performance of this engine by adding a resonance tube as a branch to connect the alternator to the loop. The efficiencies have been improved to be 23%, 59.7% and 3.5% (thermal to acoustic, acoustic to electricity, and thermal to electricity, respectively). The generated electricity has been increased to reach 13 W.

Abduljalil et al. (2009) constructed a looped tube TA engine that has a ceramic regenerator with fine square channels instead of the conventional stainless steel mesh core. The maximum measured acoustic power was about 26 W. Abduljalil et al. (2009) continued their work with some improvements and the acoustic power reached 34 W.

The multi-stage thermoacoustic engines were proposed to produce more power whenever there is enough supply of heat to be used. It was also found that the multi-stage TA engines are a solution to provide a low onset temperature (Chen, 2012). Multi-stage engines have been pioneered by de Blok (2010, 2012). Basically, they have low acoustic loss because of lower acoustic dissipation in the resonance and feedback loop. The identical multiple stages have been presented as feasible from the construction point of view because of having identical components per stage. The name "self-matching" indicates that each stage has an independent power extractor. From the losses point of view, it is better to design a self-matching engine in order to avoid high power spots and minimize losses. Four novel TA four-stage engines have been presented by de Blok (2010). All the engines have four power extraction points with productivity ranging from several watts to 1.64 kW at heat to electricity efficiency no more than 8.2%.

Some efforts towards a two-stage engine with one linear alternator have been undertaken as an outgrowth of SCORE project. Abdoulla et al. (2012) used DeltaEC to numerically design a two stage TA engine working as an electricity generator. The model gave encouraging results of 6% thermal to electricity efficiency and generating 130 W of electric power. Chen et al. (2012) built two engines: one driven by propane burner and the other by wood burner. The propane driven TA engine generated 15 W of electricity and the wood burner one produced 22.7 W. Both have used a low efficiency alternator. Kang et al. (2015) experimentally generated 204 W using a two-stage thermoacoustic looped engine with two loudspeakers. The engine found to be able to run with thermal to electric efficiency up to 3.43%.

This paper presents the experimental results of a heat driven thermoacoustic electricity generator. The system design, parts specifications and the experimental set-up will be presented first. Then the experimental results will be compared to the theoretical results which have been predicted using DeltaEC modelling tool.

II. SYSTEM CONFIGURATION

A. Overview

The current system is a one wave length thermoacoustic engine. The engine design has two stages with a Linear Alternator connected in between at two points having equal but out of phase acoustic pressure amplitudes. The connection of Linear Alternator in this configuration allows it to be run by the effect of acoustic pressure on both sides and work in a "push-pull" mode. This configuration allows the engine to have two power extraction points. The two power extraction points help to avoid high power spots and allow the stages to act as self-matching. The self-matching stages have the same identical acoustic pressure and volume flow rate amplitudes but which are out of phase. It means that each of two identical points on the two stages have the same acoustic pressure and volumetric flow velocity amplitude but shifted 180° in phase. This connection increases the system efficiency by increasing the power output and decreases the acoustic losses.

B. Modeling

To verify the idea explained in the previous section, a model has been constructed using DeltaEC. The DeltaEC shooting method showed that it was unable to run two identical stages as expected. The two identical stages when each has a power extraction point should have the same thermal and acoustical performance and this is what the shooting method failed to follow. The modelling has been done as half of the engine which is one stage and the other stage has been represented as a self-excited flow at the other side of the linear alternator.

Each thermoacoustic engine stage consists of a thermoacoustic core followed by a branch to the linear alternator and finally there is a long feedback tube. The total length of the engine is one wave length and each stage is exactly half wave length.

C. Experimental Setup

The thermoacoustic engine loop is 16 m long and uses helium at 28bar as working gas, it is illustrated in Fig 1. The thermoacoustic core consists of ambient heat exchangers AHX, regenerator, hot heat exchanger HHX, thermal buffer tube TBT and the secondary ambient heat exchanger 2ndAHX. The core has a diameter of 10cm, reduced to 7.5cm at the end of the TBT and the 2ndAXH. The core layout is shown in Fig. 2. The core is arranged vertically; the AHX at the top and the 2ndAHX at the bottom. This has been experimentally verified to enhance the temperature distribution in the regenerator and the TBT and reduce the onset temperature (Liu et. al. 2002, Abduljalil et. al. 2009).

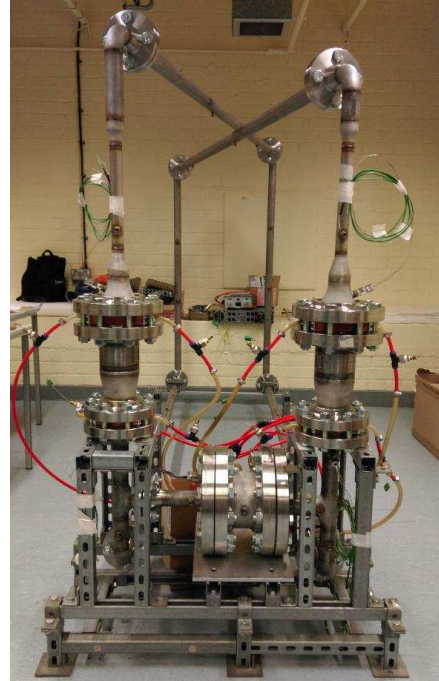


Fig. 1. Photograph of the two-stage thermoacoustic engine

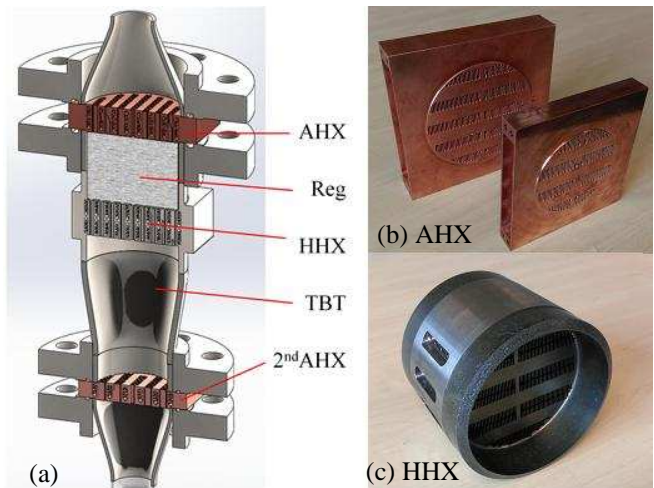


Fig. 2. (a) Thermoacoustic core (b) Ambient and secondary heat exchangers (c) Hot heat exchanger

The heat exchangers used in the model are parallel plate heat exchangers having a plate spacing of 1mm and 65% blockage ratio. The heat exchangers of this project have been fabricated using wire cutting. The wire cutting is to form tiny channels through a block of metal to form cross-

flow heat exchangers. The channels are 1mm wide leaving 0.5mm fins in between, as shown in Fig 2. Firstly, it was planned to use a simulated exhaust gases of 6.0L internal combustion engine as heat source. Unfortunately, we weren't able to do so for a laboratory limitation. Cartridge heaters have been used instead. The heaters were at a maximum power of 900W each stage. The ambient heat exchangers are water cooled to keep them at low temperature to maintain temperature difference on the hot and cold sides of the regenerator.

The AHX is of 30mm length and fabricated out of Copper. It is placed at the top of the thermoacoustic core. It consists of seven channels on the helium side and eight on the cooling water side. The regenerator is located below the AHX. It consists of 75mm thick stack of woven wire stainless steel screen punched holder with a diameter of 101mm. The diameter of the screen wire is 71 μ m. The calculated volume porosity and hydraulic radius are 75.85% and 57.5 μ m respectively. The HHX fabricated out of low carbon steel. It is 40 mm long and follows the regenerator. It has five channels on the helium.

The HHX has two collars having inner and outer diameter identical to 4" pipe of schedule40. These collars are to prevent damaging the tiny channel from damaging by the welding heat as it will be welded to a pipe and reducers to form the hot heat exchanger assembly. The thermal buffer tube TBT located between the HHX and the 2ndAHX consists of three parts: 4" diameter pipe, 4"-3" reducer, and 3" diameter pipe. The two pipes are 30mm long. The reducer of the TBT helps to suppress the Rayleigh streaming. The 2ndAHX is similar in shape and material to the AHX but it is 20mm long and 3" diameter. It has five channels on the helium side and six channels on the cooling water side.

There is a 100mm long pipe connecting the AHX to the T-branch. The T-branch is leading to a branch and a trunk. The branch is the link between the loop and the linear alternator. The trunk is 7.3m long feedback loop. The feedback loop consists of 7.05m long pipe having a diameter of 1.5" and 0.25m long pipe having a diameter of 1". The dimensions and materials of components are summarized in Table 1.

The linear alternator should have two pistons to be convenient to be used in this system. The two pistons will be located at the end of the branch of each loop. One will be subjected to positive acoustic pressure and the other to negative acoustic pressure at the same time. The positive pressure produces a push to the piston while the negative pressure produces a pull both to the same direction and hence the combined effect is a push-pull.

A Q-Drive linear alternator (Model 1S132M) has been used to convert the acoustic power to electricity. This linear alternator has one piston only. It is still useful in this application as the acoustic power can act on the piston on a side and pass through the alternator details to the other side of the piston. There is unavoidable space between the linear and the housing which acts as an acoustical compliance. This gap has been filled with a plastic inserts to reduce the effect of acoustic compliance, trying to make the two sides as similar as possible.

Table 1 Dimensions and materials summary

Component	Length (mm)	Inside Diameter (mm)	Porosity	Material
AHX	30	102.2	31.2%	Copper
Regenerator	75	102.2	75.8%	Stainless Steel
HHX	40	102.2	34.5%	Mild Steel
TBT-1 st part	30	102.2		Stainless Steel
TBT-2 nd part	102	102.2-77.9		Stainless Steel
TBT-3 rd part	30	77.9		Stainless Steel
2 nd AHX	20	77.9	31.2%	Copper
Reducer	89	40.8		Stainless Steel
Tube	100	40.8		Stainless Steel
T-branch	114	40.8		Stainless Steel
Feedback-1 st part	6800	40.8		Stainless Steel
Reducer	64	40.8-26.5		Stainless Steel
Feedback-2 nd part	275	26.5		Stainless Steel
Enlargement	166	26.5-102.2		Stainless Steel
LA Branches	200,120	40.8		Stainless Steel
LA Holder	175	154.1		Stainless Steel

D. Measurements

There are four kinds of measurements in this experiment: temperatures, pressure amplitudes, linear alternator piston displacement and generated power. There are twenty thermocouples in this rig ten in each side. In each stage, there are six measuring the Helium temperature at different locations and four measuring the change in cooling water temperatures of the ambient and secondary ambient heat exchangers. On the Helium side, there is a thermocouple in each heat exchanger and three measuring the cold side, middle and hot side temperatures of the regenerator.

The pressure amplitudes have been measured using pressure transducers. There are seventeen mounting holes accommodating PCB transducers of model 111A and 112A. The piston displacement has been measured in order to avoid damaging the linear alternator and to have an indication of the performance. The displacement has been measured by a CCD Laser Displacement Sensor. The phase difference between the piston and the adjacent pressure transducer has been recorded as well to calculate the acoustic power flowing to the linear alternator. The generated power has been calculated using the measuring values of voltage and current of the linear alternator output.

III. RESULTS AND DISCUSSION

During the experiments, system performance at 28 bar internal pressure and HHX temperature higher than 300°C were of most interest. The operating frequency was 54.68 Hz. The heat input was limited to the cartridge heaters capacity of 900W for each stage. The engine was found to run at an elevated heat loss. At "no oscillation" condition, it required 550W to keep the HHX at a temperature higher than 300°C. The study covered the three operational parameters: load resistance, mean pressure and input heat.

A. Load Resistance

The excited oscillations at a certain temperature difference push the linear alternator piston. The piston oscillation amplitude has a limit defined by the manufacturer. The piston stroke could be controlled by the resistance of the load resistance. The load resistance value affects on the generated electricity by defining the piston

stroke and the values of voltage and current. Fig 3 shows the predicted and experimental results of the output electric power as a function of the load resistance. In the experiments, a maximum generated electricity of 48.6 W was obtained at 30.8 Ω load resistance.

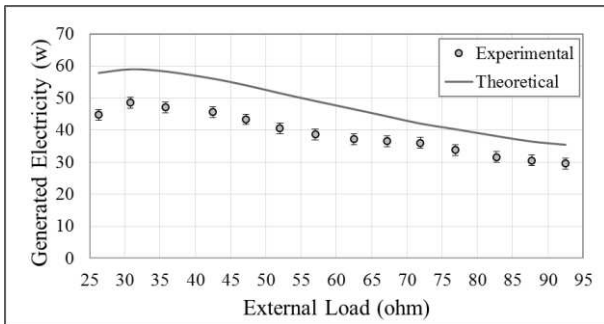


Fig. 3. The effect of load resistance on the electric power output.

B. Heat Input

It is obvious that the electricity generation of the engine is directly related to the heat input. The heat input experiments ranged from the maximum limit of 900 W to the minimum input that maintain the oscillations of 600W, all at a load resistance of 42.7 Ω . Fig. 4 shows the predicted and experimental results of the generated electric power as a function of the heat input. The temperature difference across the regenerator hasn't changed a lot by reducing the heat input from 900 W to 600 W. The main reason behind, is that reducing the heat input has damped the oscillations and hence reduced the heat transferred due to the thermoacoustic effect, as shown in Fig. 5. In this figure, the piston displacement is an example to indicate the oscillation damping.

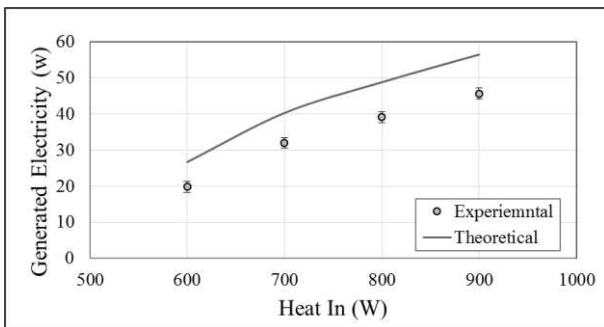


Fig. 4. Computational and experimental output electrical power as a function of Heat input.

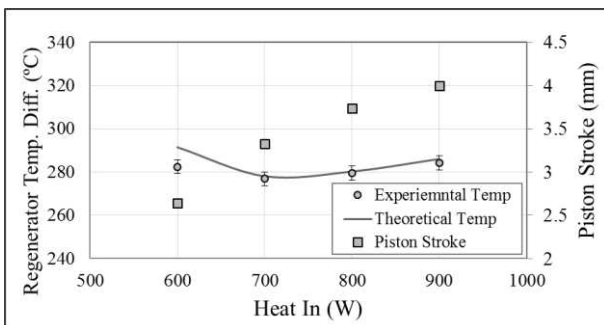


Fig. 5. Computational and experimental temperature difference across the regenerator and piston stroke as a function of load resistance.

C. Mean Pressure

The mean pressure has been studied from the maximum allowable pressure of 28 bar to the lowest pressure that runs the engine of 12 bar. The decrease in mean pressure has found to damp the oscillations, and hence decrease the generated power, pressure amplitudes, piston stroke and drive ratio. Fig 6 show the system performance at 900 W and 42.7 Ω .

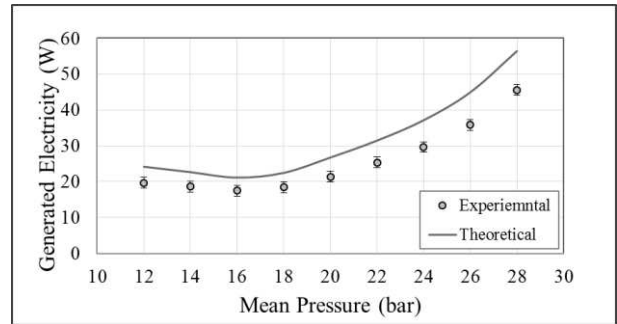


Fig. 6. Computational and experimental generated electricity as a function of load resistance.

D. Best Performance

After studying all the three operational parameters, the best performance of this thermoacoustic engine was at 30.8 Ω , 900 W heat input and mean pressure of 28 bar. In the experiments, a maximum generated electricity and heat-to-electric efficiency were 48.6 W was obtained at 30.8 Ω load resistance. The heat-to-electric efficiency was 2.7% and the oscillation frequency was 54.68 Hz. The drive ratio of 2.26% and piston stroke of 3.77 mm. The temperature difference across the regenerator was 300°C. The predicted generated electricity was 59 W leaving the agreement between the experimental and theoretical generated power to be 82.4%.

Fig. 7 illustrates the main design strategy. The strategy is to design two identical stages connected in one loop. It was targeted that the two stages have identical parts and hence they will generate and dissipate the acoustic power identically, as shown in Fig. 7e. The identical stages will have the same pressure and velocity amplitudes which will allow the connection of the linear alternator to two identical points to work in "push-pull" mode, as shown in Fig. 7a-e. The graph shows a good agreement between the calculated and measured values of the pressure amplitudes and acoustic power calculations. The only difference is around the beginning of the stages. Clearly, the second stage has higher pressure amplitude and acoustic power around the linear alternator branch as the first stage has a piston and the second stage has the back of the linear alternator as explained in the experimental set-up.

Fig. 7a shows the calculated and measured pressure amplitude distribution along the engine. There are two peaks both are near the regenerators of both stages. There is a major pressure drop at the regenerator and a minor at the linear alternator. The major one caused by the flow resistance at the regenerator and minor is due to power extraction at the linear alternator.

Fig. 7b shows the distribution of volumetric velocity along the thermoacoustic engine. Unfortunately, there is no

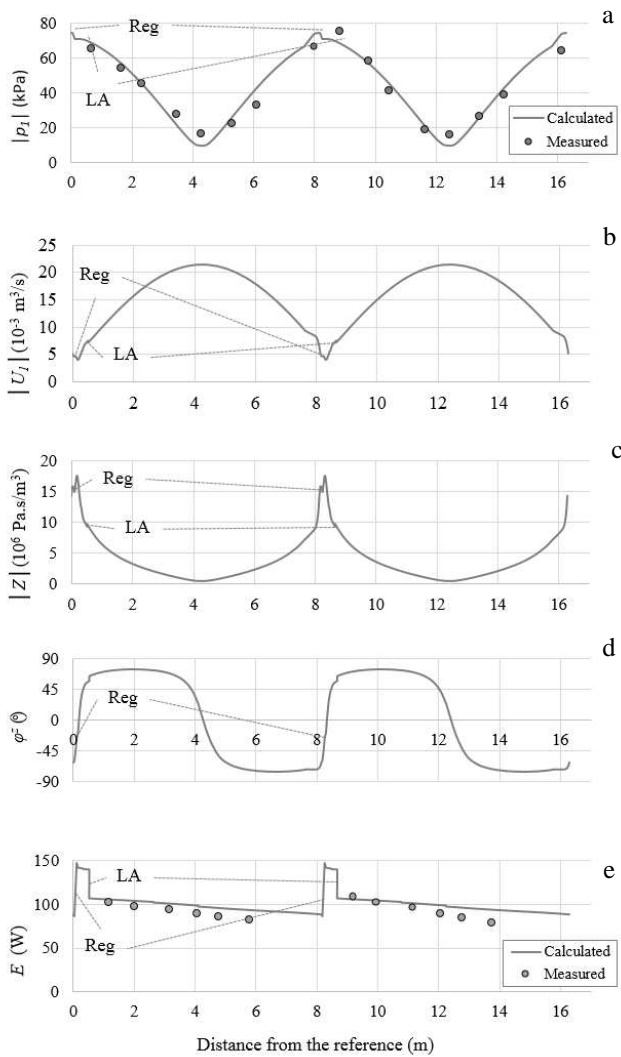


Fig. 7. (a) Pressure amplitude, (b) volumetric velocity, (c) acoustic impedance, (d) phase difference angle and (e) acoustic power flow along the engine.

velocity measurements taken in this experiments. The engine has been designed to have the lowest volumetric flow rate at the regenerator. The small volumetric flow velocity at the regenerator is essential to minimize the viscous dissipation. The effect of the temperature difference across the regenerator clearly seen in the volumetric flow rate profile as it has been increased with the regenerator limits from the cold end towards the hot end. There is a volumetric flow rate drop at the linear alternator branch caused by the power extraction at the linear alternator.

Fig.7c is the acoustic impedance profile along the engine. In simple words, the acoustic impedance is the pressure amplitude divided by the volumetric flow rate. It can be seen that the acoustic impedance is maximum at the regenerators which is one of the design strategies. The impedance drops until the middle of the feedback loop and increase again as per the fluctuation of the pressure and volumetric flow rate amplitudes.

Fig. 7d shows the phase difference between the velocity and pressure oscillation along the engine. This graph illustrates that the regenerator has been placed at near traveling-wave location. It is clear that the engine needs to be modified to have a mechanism of phase adjusting in the feedback loop.

Fig. 7e shows the acoustic power distribution along the engine. It is shown that the 86 W fed into the cold end of the regenerator, and it is amplified to 147.9 W at the hot end. The alternator extracts 33.8 W. Experimentally, both stages produced an approximate amount of the acoustic power.

There is a discrepancy between the experimental results and the theoretical data predicted by the model. There are many possible reasons. There are two main reasons and some minors.

The first main reason is that the engine runs at a huge amount of heat loss, which is not encountered in the theoretical model. The heat loss affects the engine performance rather than the discrepancy between the theoretical and experimental results only. The experiments showed that the engine cannot maintain high temperature difference across the regenerator as the drive ratio increases. The main source of heat loss is that the AHX and 2ndAHX are in metal-to-metal contact to the HHX assembly, as they are sealed using o-rings. This heat leak will be eliminated in future work by replacing the o-rings with relatively low conductivity gaskets.

The second main reason may be streaming. The temperature gradient across the regenerator and the elevated mean pressure excite a superimposed type of flow usually called streaming. This kind of flow is considered to be a steady mass flow. This phenomenon is responsible for dissipating energy as it involves heat transfer to the wall within the regenerator limit (Paridaens et. al. 2013, S. Job et. al. 2003). This effect of the streaming could be seen in Fig 8. It is showing the temperature distribution in the regenerator in three difference locations: cold end, middle and hot end, at different load resistance. Theoretically, temperature distribution across the regenerator should be linear. The streaming effect is responsible of non-linear temperature distribution in the graph. Another point to make here is that the streaming/non-linear temperature distribution is worse at higher resistance. This could be interpreted as increasing the load resistance will increase the drive ratio. In other words, the higher the drive ratio is the higher streaming effect will appear. Fig. 9 and 10 show the effect of the load resistance on the drive ratio and temperature difference across the regenerator.

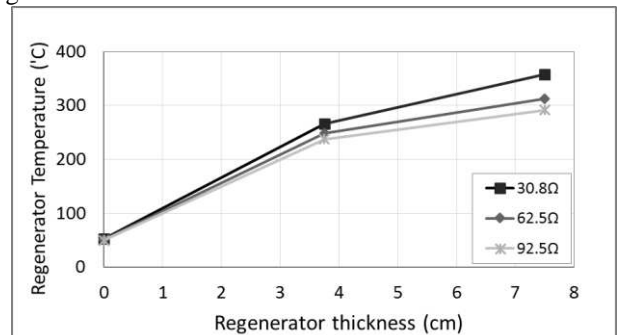


Fig. 8. Temperature distribution across the regenerator at different load resistance.

More experiments will be done later to suppress the streaming by placing an elastic membrane at a low volumetric flow rate.

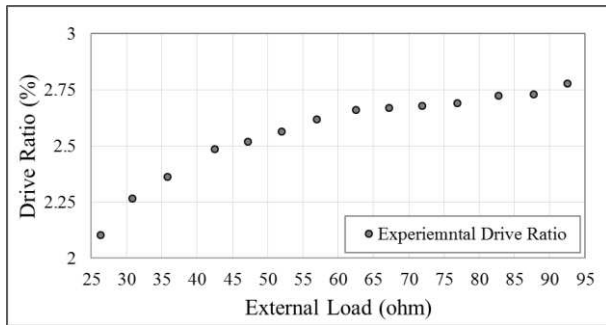


Fig. 9. Experimental drive ratio at different load resistance.

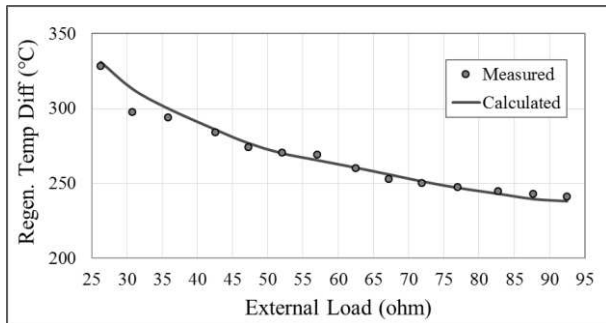


Fig. 10. Measured and calculated temperature difference across the regenerator at different load resistance.

Two of the minor discrepancy sources are the modelling code and the dimensions of the physical parts. The DeltaEC modeling code is a one-dimensional linear thermoacoustic representation that does not consider any non-linear, two dimensional or three-dimensional effects. In experiments, there are many of these effects. The physical parts making the engine do not perfectly match the modeled dimensions. The other main issue related to the physical parts is the guessed value of the smoothness of the inner diameter of the tubes, there isn't a certain value.

IV. CONCLUSION AND FUTURE WORK

A thermoacoustic engine runs a linear alternator in a "push-pull" mode, working at a frequency of 54.68 Hz, was designed and tested in this study. The system performance was investigated at different resistive load, mean pressure and heat input. The maximum generated power and thermal-to-electric efficiency of 48.6 W and 2.7% respectively, at 30.8 Ω resistive load and 28 bar mean pressure. The test of the thermoacoustic engine showed that it needs to be amended to reduce the heat loss and suppress the streaming. The heat loss will be reduced by placing a gasket between the AHX and the HHX assembly. The gasket expected to apply heat insulation as well as pressure sealing. The streaming will be eliminated by placing a membrane in a suitable location.

Acknowledgment

A. Hamood would like to acknowledge the Human Capacity Development Program (HCDP) sponsored by Kurdistan regional government. A.J. Jaworski would like to acknowledge Royal Society Industry Fellowship funding.

References

[1] Abdoulla K., Yu, Z. & Jaworski A.J., 2012. Design of a Low-Cost Two-Stage Thermoacoustic Electricity

Generator For Rural Communities In Developing Countries. In ICSV19. pp. 1–8.

[2] Abdoulla K., Kang H. & Jaworski A.J., 2013. Travelling wave thermoacoustic electricity generator for rural areas using a side-branch alternator arrangement. In World Conference of Engineering.

[3] Abduljalil A.S., Yu Z. & Jaworski A.J., 2009. Construction and Performance Characterization of the Looped-Tube Travelling-Wave Thermoacoustic Engine with Ceramic Regenerator. International Journal of Engineering and Applied Sciences, 5:3, pp.139–143.

[4] de Blok C.M., 2010. Novel 4-Stage Traveling Wave Thermoacoustic Power Generator. In ASME 2010 3rd Joint US-European Fluids Engineering Summer Meeting and 8th International Conference on Nanochannels, Microchannels, and Minichannels. pp. 1–8.

[5] de Blok C.M., 2012. Multi-Stage Traveling Wave Thermoacoustics In Practice. In ICSV19. pp. 1–8.

[6] Ceperley P.H., 1979. A pistonless Stirling engine-The traveling wave heat engine. J. Acoustical Soc. Am., 66,1508-1513.

[7] Chen B., 2012. Development and Assessment of Thermoacoustic Generators Operating by Waste Heat from Cooking Stove. Engineering, 04(12), pp.894–902.

[8] H. Liu, E. Luo, H. Ling, J. Wu . (2002). The Influence of Thermal Natural Convection on a Traveling-Wave Thermoacoustic Engine. Cryocoolers . 12 (2), 447-450.

[9] Huifang Kang, Peng Cheng, Zhibin Yu and Hongfie Zheng, (2015). A two stage traveling-wave thermoacoustic electric generator with loudspeakers as alternators. Applied Energy 137 (2015) 9-17.

[10] Job J., Gusev V., Lotton P. and Bruneau, M., (2003). Acoustic streaming measurements in annular thermoacoustic engines. J Acoust Soc Am. 2003 Apr;113(4 Pt 1):1892-9.

[11] Paridaens R., Koudri S., and Jerbi F., (2013). Investigation on the generation mechanisms of acoustic streaming in a thermoacoustic prime mover. Cryogenics 58 (2013) 78–84

[12] Sakamoto S. & Watanabe Y., 2006. Experimental study on resonance frequency of loop-tube-type thermoacoustic cooling system. Acoustical Science and Technology, 27(6), pp.361–365.

[13] Sakamoto S., Sahashi K. & Watanabe Y., 2012. Improving Thermoacoustic System Efficiency, Measurement of a Sound Field in the Phase Adjuster. Proceedings of Symposium on Ultrasonic Electronics, 33, pp.215–216.

[14] Swift G., 2001. Thermoacoustic: a unifying perspective for some engines and refrigerators Fifth draf., Los Almos National Laboratory.

[15] Yu Z. & Jaworski A.J., 2012. Demonstrator of a combustion driven thermoacoustic electricity generator for remote and rural areas of developing countries. In ICSV19. pp. 1–8.